Scanning Force Microscopy of Gypsum Dissolution and Crystal Growth

Christopher Hall
Schlumberger Cambridge Research, Cambridge CB3 0EL, United Kingdom

David C. Cullen
Institute of Biotechnology, University of Cambridge, Cambridge CB2 1QT, United Kingdom

Dissolution and crystal growth on the (010) cleavage surface of mineral gypsum have been studied by scanning force microscopy, which allows observation of surfaces while they are in contact with aqueous solutions. Etch pits formed on the (010) surface in contact with solutions undersaturated with respect to gypsum are oriented in relation to the [001] zone axis. Edges parallel to [001] are stable or move only slowly. Edges parallel to [100] and [101] move more rapidly. Crystal growth by migration of step edges is observed in contact with supersaturated solutions. The inhibition of crystal growth by phosphonate produces gross changes in the texture of steps and terraces.

Introduction

Scanning (or atomic) force microscopy (SFM) has recently been used to study mineral surfaces in contact with aqueous solutions, notably by Hansma and coworkers (Gratz et al., 1993; Hillner et al., 1992, 1993), and Hochella and coworkers (Johnsson et al., 1991; Dove and Hochella, 1993). The technique seems certain to become a versatile tool for studying dissolution and crystal growth processes which are of wide interest in industrial mineral processing, aqueous geochemistry and environmental chemistry. SFM generates a real-space topographic image of a surface with high resolution both laterally and vertically. This is achieved by bringing a microscopic probe into contact with the sample and rastering it across the sample surface using piezoelectric actuators while maintaining (most commonly) a constant probe-sample interaction force. This force determines the deflection of the cantilever with which the probe is integrated and the deflection is measured using a laser beam optical lever and quadrant photodetector. The photodetector output is used in a feedback loop to control the z piezoelectric actuator. Positional information from the piezos is used to construct a three-dimensional image of the sample surface. SFM, together with scanning tunneling microscopy (STM), form the main implementations of a large class of scanning probe microscopies (Wiesendanger, 1994).

SFM has a number of valuable features for the study of crystal surface processes. These are easy sample preparation, ability to image in both air and liquid environments, imaging of nonconducting surfaces, many tip/surface imaging modalities, and micron to atomic scale xy resolution, combined with subnanometer z resolution. Limitations include the need to work on surfaces which are reasonably flat (defined as a z range expressed as some function of the probe geometry) and lack of direct chemical identification of surface materials.

This article reports results from an exploratory study to assess the use of SFM in materials chemistry for oilfield engineering. Gypsum was selected as a cleavable mineral which is one of the main inorganic scales deposited in hydrocarbon reservoirs. Gypsum also plays a critical role in the hydration chemistry of oilwell cements and is known to be subject to crystal growth inhibition by some substances which act as cement set retarders. Gypsum is arguably the most important of all cement additives, being universally added to commercial Portland cements to suppress the rapid hydration reaction of calcium aluminate. Dissolving gypsum flushes calcium and sulfate ions into solution within seconds of first wetting the cement. Thereafter, the chemical interplay of clinker and sulfate minerals dominates the early hydration of all portland cements.

Correspondence concerning this article should be addressed to C. Hall.
Current address of D. C. Cullen: Biotechnology Centre, Cranfield University, Cranfield, Bedfordshire, MK43 0AL, United Kingdom.

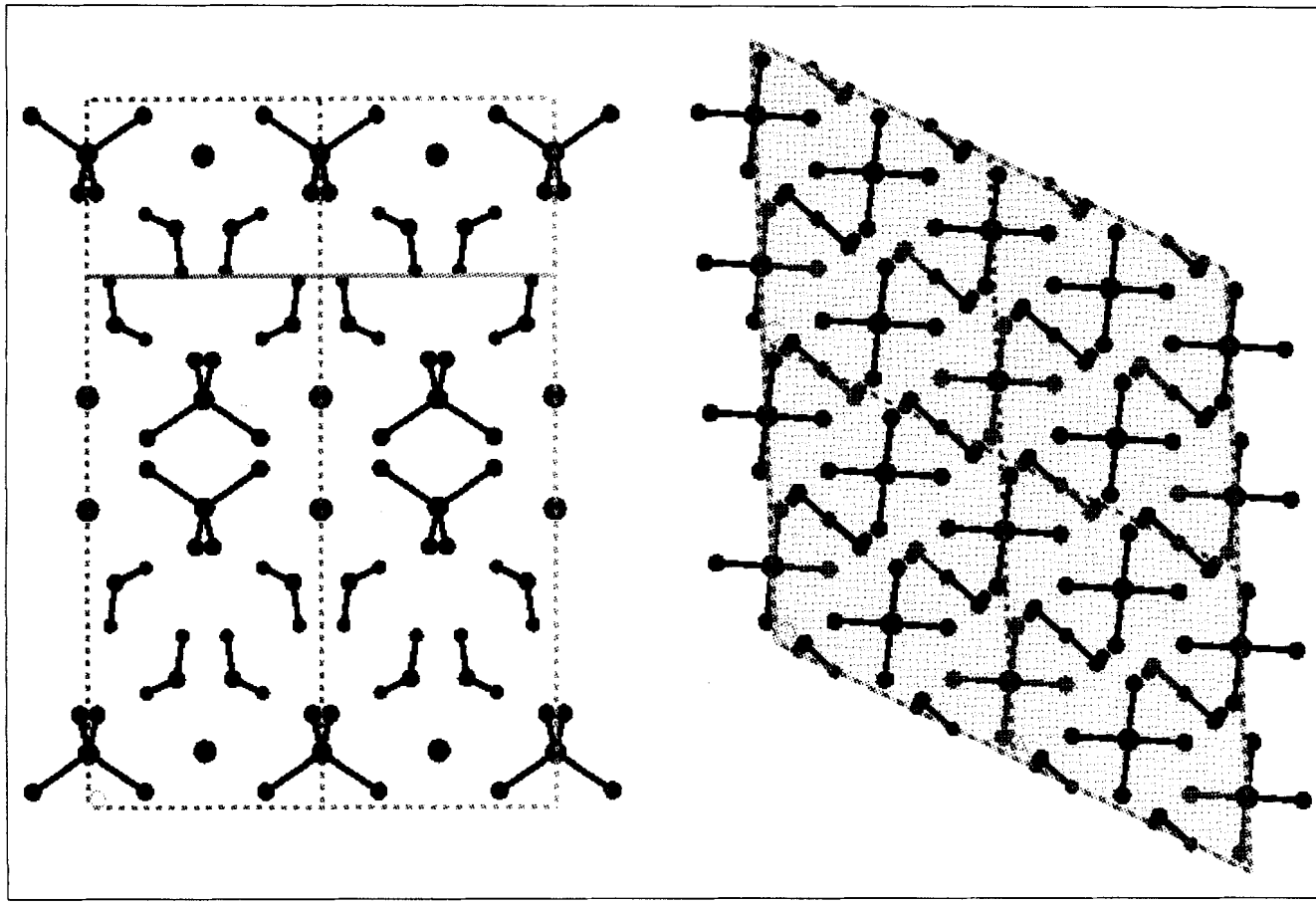

Figure 1. Unit cell of gypsum (Pederson and Hemmingsen, 1982): $a = 0.5679$; $b = 1.5202$; $c = 0.6522$ nm; $\beta = 118.43°$; space group I2/a.

Left: projection on the (001) plane; showing the cleavage surface between planes of water molecules at $y = 0.75$. *Right*: projection on the (010) plane.

Materials: Gypsum

The samples used were taken from a large single crystal geological specimen of good clarity. Gypsum $CaSO_4.2H_2O$ has a monoclinic crystal structure (neutron diffraction refinement by Pederson and Hemmingsen, 1982) and cleaves readily parallel to its (010) lattice plane. This plane is parallel to double sheets of water molecules between which there is only weak H-bonding (see Figure 1 for crystallographic data). In fact cleavage is so easy that samples require some care in preparation to avoid separation along several cleavage planes simultaneously. Individual crystal samples, typically $2 \times 2 \times 0.3$ mm, were mounted on 8-mm-dia. stainless steel disks using a graphite-filled adhesive and edge sealed with acrylic varnish. Two of the many crystals studied were also indexed by standard X-ray precession camera methods to establish the directions of the a and c axes. Solutions supersaturated and undersaturated with respect to gypsum were prepared by mixing and diluting calcium chloride and sodium sulfate stock solutions (both 0.108 M). We use the quantity $\sigma = (c - c_s)/c_s$ to describe the relative supersaturation of the solutions used. Here c is the concentration of calcium sulfate and c_s the solubility of gypsum. c_s is about 2.55 g/L at 25°C in pure water (Knacke and Gans, 1977). At saturation, $\sigma = 0$; $\sigma < 0$ describes undersaturated solutions and $\sigma > 0$ supersaturated solutions.

Scanning Force Microscopy

SFM images were acquired using a TopoMetrix TMX 2000 scanning probe microscope fitted with an SFM head and standard TopoMetrix SFM probes (force constant about 0.032 N/m) and operating in constant force (contact) mode with a typical applied force of 10 nN. The images shown are constructed from either 400×400 or 200×200 pixel datasets. Raw data are z displacements, but we show processed images as top views with apparent left-to-right illumination applied. The probe speed across the sample is 20–100 μm/s in the fast scan direction, so that image acquisition times are typically 30–50 s. Most images were acquired with a 25-μm range scanner with the sample in contact with aqueous solutions. For this the sample is enclosed in a cell (capacity approximately 1.25 mL) fitted with inlet and outlet ports and sealed below with a soft rubber membrane. The solutions can be changed without demounting the sample using syringes or by gravity feed via a vernier controlled needle valve, giving flow rates of 10–100 μL/s. Likewise, slow flow through the cell

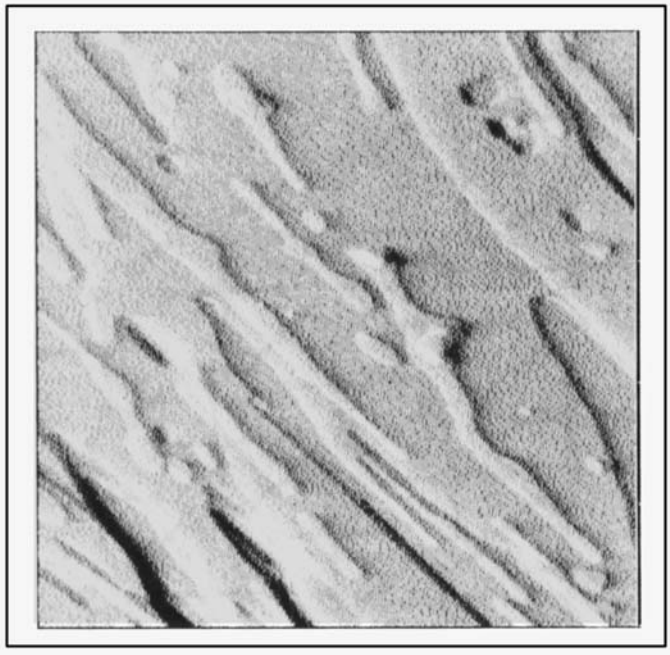

Figure 2. Gypsum (010) cleavage surface imaged in air; image field 6.55 μm $\times$ 6.55 μm.

during imaging provides laminar flow across the sample surface and maintains steady bulk concentrations for any diffusion controlled processes acting on the sample. All the experiments described were carried out at room temperature (about 20°C).

Observations of the (010) Surface

The dry freshly cleaved material imaged in air shows atomically flat terraces, with ragged steps and some isolated debris (Figure 2). The step edges do not show marked crystallographic orientation, although some directionality is evident. The steps are mostly *elementary*, having a height corresponding approximately to the b dimension of the unit cell (0.7–0.8 nm as measured). The surface is stable in air, at least over periods of hours.

Dissolution

To observe dissolution, samples were brought into contact with undersaturated calcium sulfate solutions. For $\sigma < -0.05$, we observe a relatively high level of activity on the surface, such that easily measurable changes occur between successive imaging scans: typically 50 s per frame. Figure 3 shows a dissolution sequence extending over about 15 min. and showing the same surface as in Figure 2.

Over the first few minutes of contact between a freshly cleaved surface and an undersaturated solution, the surface structure cleans up substantially. Isolated and exposed elevated regions disappear within seconds. Ragged and curved steps etch back, stabilizing along one particular crystallographic direction. This direction was shown to be the [001] zone axis on an independently indexed sample. The overall effect of the initial dissolution is to create a much cleaner and more geometrical topography. The stable steps once es-

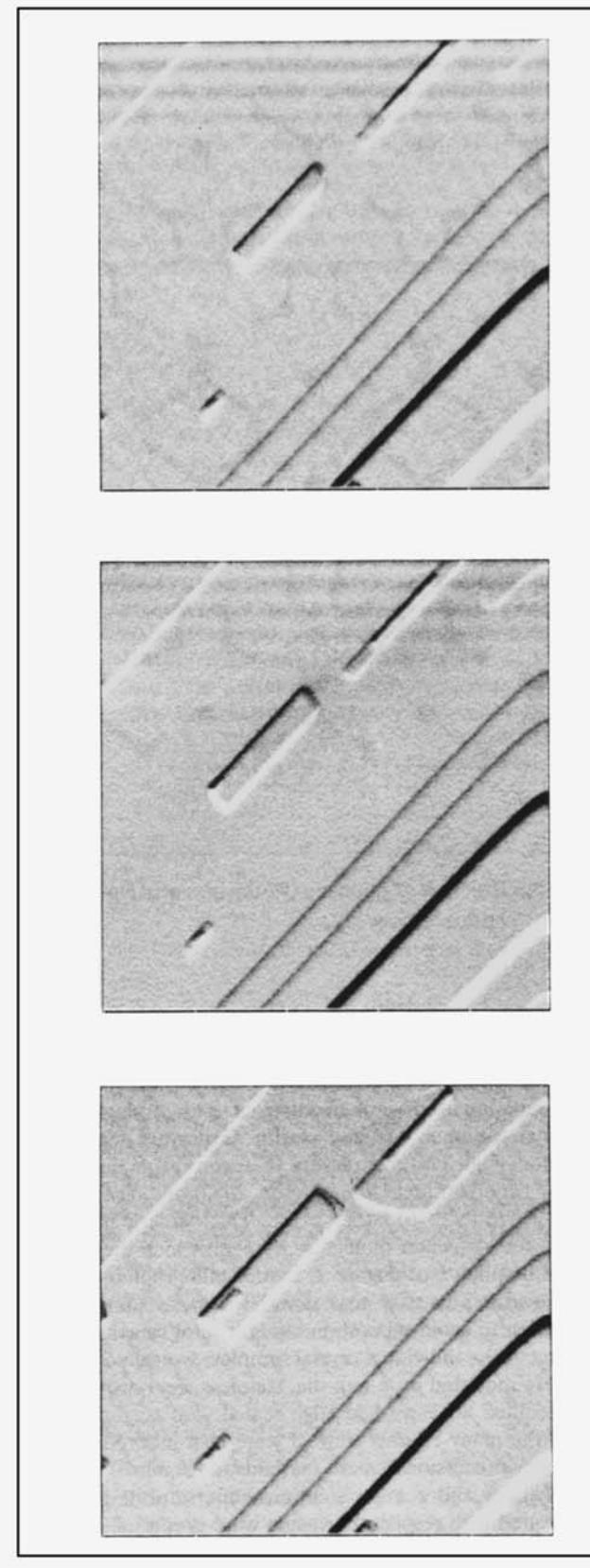

Figure 3. Dissolution sequence, gypsum sample in Figure 2 in contact with nonflowing calcium sulfate solution, $\sigma = -0.05$.

Image field, 5 μm $\times$ 5 μm; acquisition time, 50 s; images at 7-min intervals, starting 30 min after contact with solution.

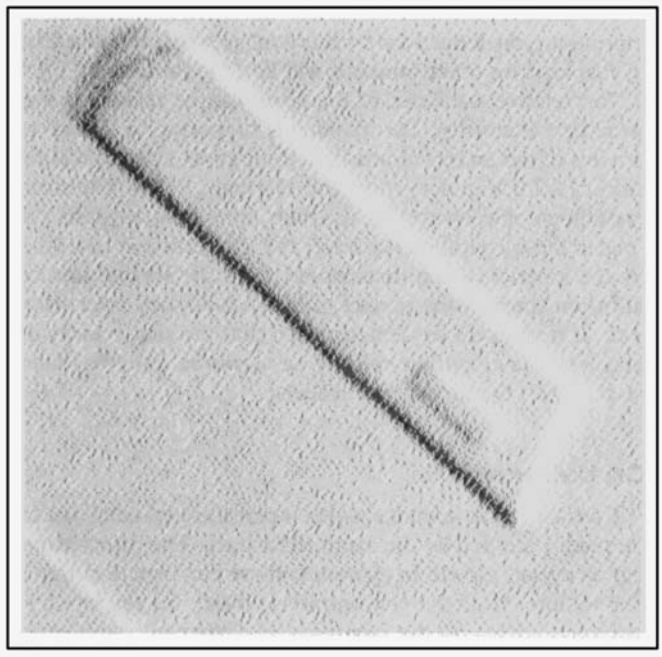

Figure 4. Pit morphology: enlargement of central pit in Figure 3 (*right*).

Image field 2,175 nm×2,175 nm.

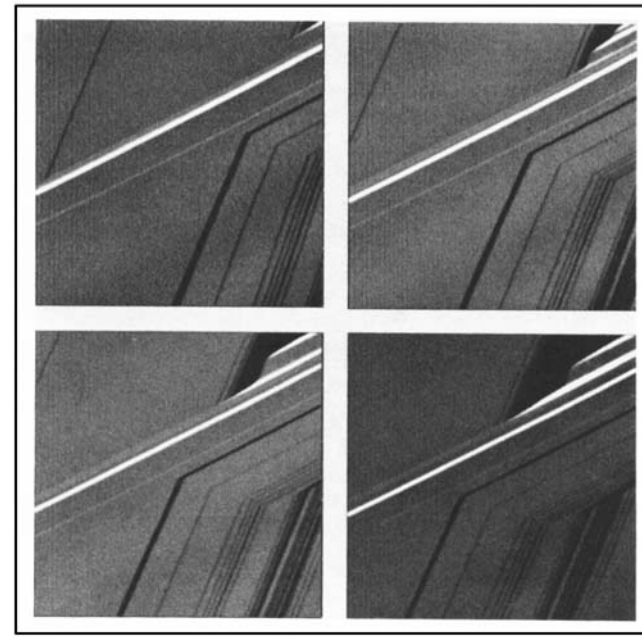

Figure 5. Dissolution sequence: image field 10 μm×10 μm, 1-min interval.

tablished remain essentially stationary. However, a second striking feature is the sudden appearance of etch pits. These are in the form of long, almost rectangular trenches, aligned along the same direction as the stable steps. These pits appear completely formed within the period of a single scan; thereafter, they remain stable for many minutes. We note that pits formed at low undersaturations often have a small core cavity (Figure 4).

After the initial cleanup, the surface takes on a highly geometrical appearance. Figure 5 shows a dissolution sequence extending over a period of about 10 min at $\sigma = -0.1$. All steps are aligned along two directions and continued etching occurs by retreat of these steps. The step velocity is constant (as is clearly shown by the straightness of the edges in the SFM image) but differs greatly in the two directions. In the case of the series of images shown in Figure 5, the velocity of the faster moving step is about 13.0 nm/s; while that of the slower moving step is almost zero, certainly not more than 0.75 nm/s (Figure 6). These values are similar to those recently reported by Bosbach and Rammensee (1994) for gypsum dissolution (with sodium nitrate rather than sodium chloride as the background electrolyte).

The apparent step velocity measured directly from the image has to be corrected for the finite raster speed in the slow scan direction: in this case, the raster speed is about 185 nm/s and the simple trigonometrical correction (Hillner et al., 1992) is small.

Crystallography of the etch pits

The slow (almost stable) edges of the etch pits are invariably aligned with the [001] zone axis. The orientation of the faster moving face is more variable and appears to depend on the undersaturation. The pit angle is approximately 115–120°, with the shorter edge of the pit aligned approximately along [100]; the obtuse edge pit corners are usually rounded (Figures 3 and 4). (Rounded *growth* morphologies are generally

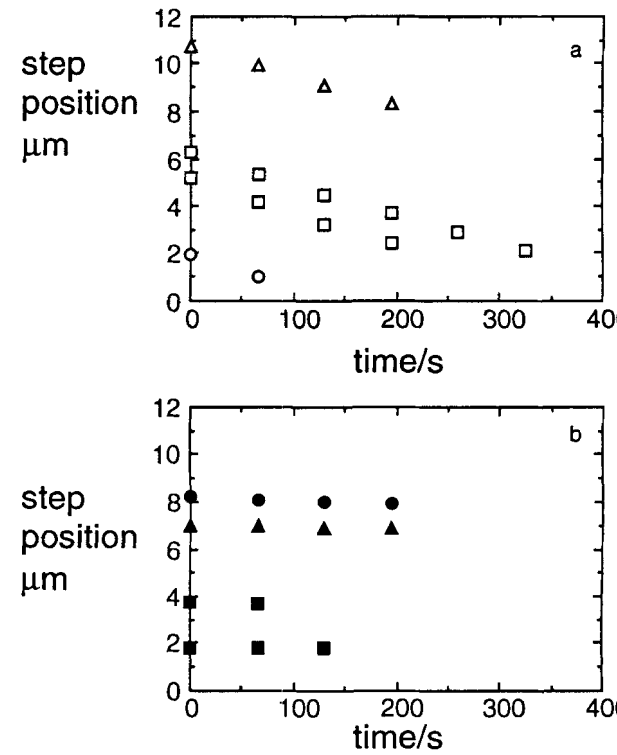

Figure 6. Step motion: displacement of fast and slow step edges (Figure 5) with trigonometrical correction for finite raster speed.

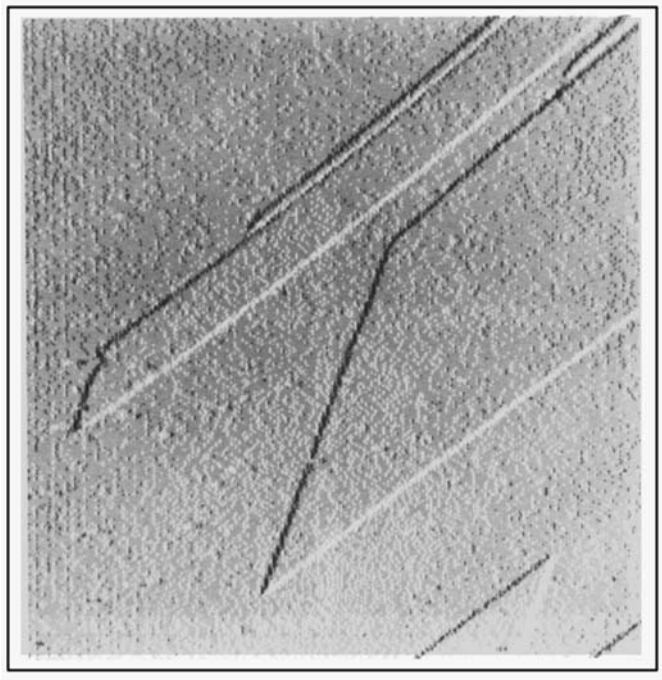

Figure 7. Dissolution etching: image field 11.5 μm× 11.5 μm.

associated with the absence of strong crystallographic differentiation in the attachment rates and for etching presumably likewise in detachment rates. Stipp et al. (1994) note similar rounding in etch pits on calcite.) At somewhat higher etching rates, the rounding of the angle disappears and alignment of the faster moving edge is usually more parallel to [101], as shown in Figure 5. Here the image field is dominated by a stable multiple step extending diagonally from the top right-hand corner. This is an [001] step edge which moves only very slowly downwards. Etching occurs mainly by the much faster movement of mostly elementary steps migrating from right to left. The series of step edges which now occupy the bottom righthand quadrant of the field can be seen to move rapidly to the left, while precisely maintaining their relative positions. Meanwhile, the complex pit at the top right steadily deepens.

At greater undersaturations ($\sigma = -0.5$, for example) the etch pits or angle of intersection of the steps may become still more sharply angled (Figure 7). The slow or stable edge remains oriented along [001] but the faster moving edge shifts its orientation towards [102] as σ decreases.

These crystallographic observations are consistent with the relative stability of the crystal faces of gypsum deduced from the morphology of gypsum single crystals grown from solution. Such studies (for example, van Weijnen et al., 1987a) show that the most stable faces are (010) and (120), while (011) and (111) are fast growing and less stable. In the SFM image, we observe the (010) face. On this face, the (120) lattice plane lies in the [001] zone, which we observe to be very slow moving and stable during dissolution. The (011) plane on the other hand lies in the [100] zone which is unstable. Finally, the (111) plane lies in the [101] zone, which we observe becomes the preferred direction for rapid etching at greater undersaturation. The consistency of our kinetic SFM observations of the gypsum surface during dissolution and the morphological deductions from crystal growth is notable. Data of this kind on other minerals will be of great interest.

The relative stabilities of the edges can be related to their structural chemistry. This ranking is supported by several estimates of the energy of attachment of growth slices (Weijnen et al., 1987a; Van der Voort and Hartman, 1991). The strong crystallographic control of the step movement suggests that (under these conditions at least) the dissolution is controlled by the kinetics of ion detachment from the surface and not diffusion through the surface/solution boundary layer. However, it remains to be demonstrated that the step velocity depends on the cross-flow velocity [as shown recently by Manne et al. (1993) for certain aminoacids].

Crystal Growth

Crystal growth in contact with supersaturated solutions can be readily studied by the same techniques. The phenomenology of crystal growth in gypsum is more complex than that of dissolution. At all the concentrations which we employed, we observed growth by the migration of elementary steps across the field of view. Even at the lowest supersaturations, we did not observe growth spirals of the kind originally proposed by Burton, Cabrera and Frank (1951) and shown in an SPM study by Gratz and Hillner (1993) to occur on calcite. This surprising finding however agrees with the recent study of Bosbach and Rammensee (1994). The nucleation and growth on gypsum surfaces clearly requires more detailed investigation, since a spiral growth mechanism was inferred by Christoffersen et al. (1982) from an analysis of gypsum crystallization kinetics.

At low supersaturations, the migrating steps were elementary and well separated. In most cases, a series of steps migrated at roughly constant rate, so that the spacing between steps was maintained, at least over short distances and periods of time. An example is shown in Figure 8, where the step spacing is about 0.5 μm. In nearly all cases, the growth step edges were somewhat ragged and crystal growth did not show the strong crystallographic orientation observed in dissolution.

Inhibition

It is well known (Liu and Nancollas, 1975) that soluble phosphonates retard (and at higher concentrations inhibit) the seeded crystallization of gypsum in contact with supersaturated solutions. Phosphonates also retard portland cement hydration (Ramachandran et al., 1993), probably through interaction with complex calcium sulphoaluminate hydrates. Figure 9 shows the effect of adding 50 ppm of ethylenediaminetetra(methylenephosphonic) acid (as Dequest 2041 from Monsanto) to the aqueous phase of a supersaturated solution ($\sigma = 1.0$) during crystal growth of gypsum. The sequence shown covers a period of some 10 min. The immediate effect of adding phosphonate is to halt the overall uniform forward motion of the steps. The steps become ragged as short lengths of the step break out and move a short distance forward, only in turn to be stopped. The result is that the steps become crenellated, with the scale of the crenellation becoming finer with time. After some 10 min all activity is killed. The charac-

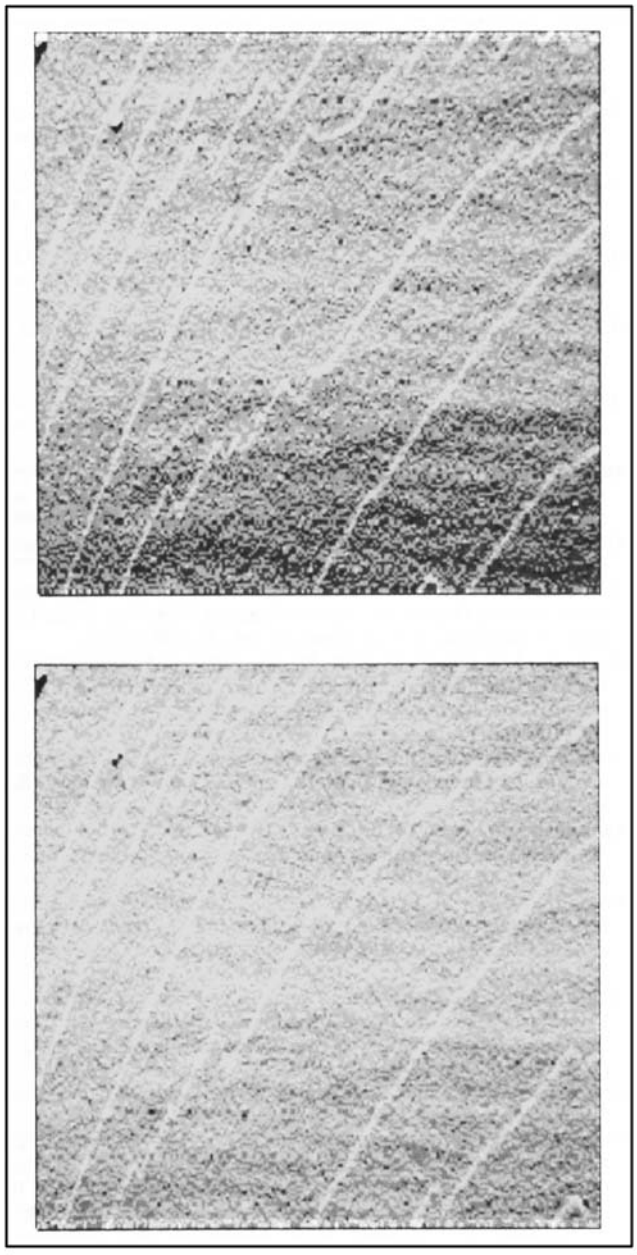

Figure 8. Crystal growth-sequence: image field 20 μm $\times$20 μm, frames at 2-min interval.

Note asperities at the top left as location markers.

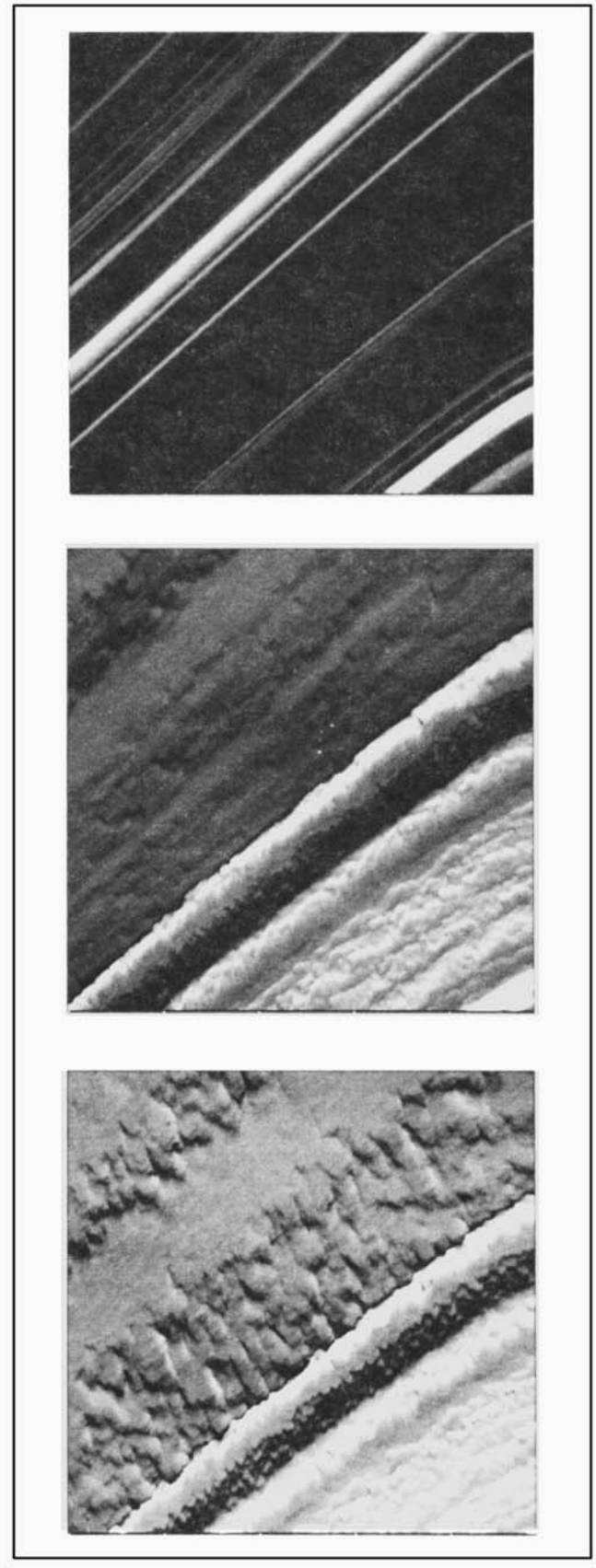

Figure 9. Inhibition of crystal growth by phosphonate: σ = 0.3, 50 ppm.

Image field 5.87 μm $\times$ 5.87 μm; images at 4-min intervals.

teristic length of the fine structure of the inhibited edge is 100–200 nm (Figure 9).

These observations seem to be consistent with the view (see discussion of Weijnen et al., 1987b) that inhibition occurs by adsorption of inhibitor molecules at kink sites in the steps. Once adsorbed, the blocked kink site becomes inactive. New kink sites can be generated spontaneously at the edge, which can grow provided that the length of the free edge is greater than the critical nucleation distance. Once inhibitor molecules have been adsorbed in sufficient numbers, no further nucleation is possible. We can compare our observations with the theoretical analysis of Weijnen et al., who estimated the kink site density and step spacing for various faces of gypsum. For

the (010) face, the estimated values were quite similar for the [100] and [001] steps: kink spacing 200–400 nm, step spacing 300–500 nm. The critical nucleation radius was about 20 nm. We cannot make any precise comparisons but note that the elementary step spacing in Figure 8 is also about 500 nm. while the characteristic length for the fine structure of the inhibited steps in Figure 9 is around 150 nm. This can hardly be greater than the kink spacing and must be greater than the nucleation radius, as it is seen to be in this case (Figure 9), with the caution that we are here observing multiple steps.

The general texture of the surface after crystal growth has stopped is similar in some respects to that of calcite poisoned by sodium dihydrogen phosphate as described by Hillner et al. (1992).

Conclusions

The work reported indicates some of the capabilities of SFM in crystallization research. We provide new data on the crystallographic control of gypsum dissolution on the (010) face. Dissolution occurs by formation and development of crystallographically oriented etch pits. The relative rates of etching of the [100] and [001] steps correspond to the known stability of certain faces during crystal growth. In crystal growth, we observe directly the microstructural or textural effects of a phosphonate inhibitor acting on growing steps. In both cases, SFM imaging provides *in-situ* dynamic information of both quantitative and quantitative value.

SFM provides a means of observing changes on mineral surfaces during crystal growth and dissolution of remarkable power. For research on surface chemistry and crystallization, the ability to image continuously while controlling flow and mass transfer across the sample surface remains largely unexploited.

Acknowledgments

We thank Sally Colston and Jezz Leckenby for their valuable contributions.

Literature Cited

Bosbach, D., and W. Rammensee, "In situ Investigation of Growth and Dissolution on the (010) Surface of Gypsum by Scanning Force Microscopy," *Geochim. Cosmochim. Acta*, **58**, 843 (1994).

Burton, W. K., N. Cabrera, and F. C. Frank, "The Growth of Crystals and the Equilibrium Structure of their Surfaces," *Phil. Trans. Roy. Soc. London*, **A243**, 299 (1951).

Christoffersen, M. R., J. Christoffersen, M. P. C. Weijnen, and G. M. Van Rosmalen, "Crystal Growth of Calcium Sulphate Dihydrate at Low Supersaturation," *J. Cryst. Growth*, **58**, 585 (1982).

Dove, P. M., and M. R. Hochella, Jr., "Calcite Precipitation Mechanisms and Inhibition by Orthophosphate: in situ Observations by Scanning Force Microscopy," *Geochim. Cosmochim. Acta*, **57**, 705 (1993).

Gratz, A. J., and P. E. Hillner, "Poisoning of Calcite Crystal Growth Viewed in the Atomic Force Microscope (AFM)," *J. Cryst. Growth*, **129**, 789 (1993).

Gratz, A. J., P. E. Hillner, and P. K. Hansma, "Step Dynamics and Spiral Growth on Calcite," *Geochim. Cosmochim. Acta*, **57**, 491 (1993).

Hillner, P. E., S. Manne, A. J. Gratz, and P. K. Hansma, "AFM Images of Dissolution and Growth on a Calcite Crystal," *Ultramicroscopy*, **42–44**, 1387 (1992).

Hillner, P. E., S. Manne, A. J. Gratz, and P. K. Hansma, "The AFM: a New Tool for Imaging Crystal Growth Processes," *Faraday Discuss.*, **95**, 191 (1993).

Hillner, P. E., A. J. Gratz, S. Manne, and P. K. Hansma, "Atomic-Scale Imaging of Calcite Growth and Dissolution in Real Time," *Geology*, **20**, 359 (1992).

Johnsson, P. A., C. M. Eggleston, and M. F. Hochella, Jr., "Imaging Molecular-Scale Structure and Microtopography of Hematite with the Atomic Force Microscope," *Am. Mineralogist*, **76**, 1442 (1991).

Knacke, O., and W. Gans, "The Thermodynamics of the System $CaSO_4$-H_2O," *Zeitschrift für Physikalische Chemie*, **104**, 41 (1977).

Liu, S. T., and G. H. Nancollas, "A Kinetic and Morphological Study of the Seeded Growth of Calcium Sulphate Dihydrate in the Presence of Additives," *J. Coll. Interface Sci.*, **52**, 593 (1975).

Manne, S., J. P. Cleveland, G. D. Stucky, and P. K. Hansma, "Lattice Resolution and Solution Kinetics on Surfaces of Amino Acid Crystals: An Atomic Force Microscope Study," *J. Cryst. Growth*, **130**, 333 (1993).

Pederson, B. F., and D. Semmingsen, "Neutron Diffraction Refinement of the Structure of Gypsum $CaSO_4.2H_2O$," *Acta Cryst.*, **B38**, 1074 (1982).

Ramachandran, V. S., M. S. Lowery, T. Wise, and G. M. Polomark, "The Role of Phosphonates in the Hydration of Portland Cement," *Mater. Str.*, **26**, 425 (1993).

Stipp, S. L. S., C. M. Eggleston, and B S. Nielsen, "Calcite Surface Structure Observed at Microtopographic and Molecular Scales with Atomic Force Microscopy (AFM)," *Geochim. Cosmochim. Acta*, **58**, 3023 (1994).

Weijnen, M. P. C., G. M. van Rosmalen, P. Bennema, and J. J. M. Rijpkema, "The Adsorption of Additives at the Gypsum Crystal Surface: I. Determination of the Interfacial Bond Energies," *J. Cryst. Growth*, **82**, 509 (1987a).

Van der Voort, E., and P. Hartman, "The Habit of Gypsum and Solvent Interaction," *J. Cryst. Growth*, **112**, 445 (1991).

Weijnen, M. P. C., G. M. van Rosmalen, and P. Bennema, "The Adsorption of Additives at the Gypsum Crystal Surface: A Theoretical Approach. II. Determination of the Surface Coverage Required for Growth Inhibition," *J. Cryst. Growth*, **82**, 528 (1987b).

Wiesendanger, R., *Scanning Probe Microscopy and Spectroscopy*, Cambridge Univ. Press, Cambridge, U.K. (1994).

Manuscript received Dec. 27, 1994, and revision received Mar. 20, 1995.